

Mathematical Modelling of an Enzymatic Separating Microreactor*

F. TMĚJ, P. HASAL**, Z. LIMBERGOVÁ, R. CHMELÍKOVÁ, and M. MAREK

*Department of Chemical Engineering & Center for Nonlinear Dynamics of Chemical and Biological Systems,
Institute of Chemical Technology, CZ-166 28 Prague
e-mail: Pavel.Hasal@vscht.cz*

Received 18 April 2001

A microreactor—separator system constructed of thin channel filled with an enzyme and microparticulate solid adsorbent immobilized in hydrophilic gel was studied by numerical simulations using a mathematical model of the reactor system. A substrate-inhibited enzyme reaction producing two nonionic products from nonionic substrate (*e.g.* sucrose hydrolysis by invertase) was considered. Electroosmotic flux and molecular diffusion were considered as mass-transport processes in the gel, as no electrophoretic migration was possible. The mathematical model involved the mass balances of all reaction components in liquid and solid phases, enthalpy balance, and equation describing the enzyme inactivation. A periodic switching of the substrate concentration at the reactor inlet, resulting in periodic alternation of reaction and separation periods, was applied. Dependences of the microreactor—separator operating measures (*e.g.* separation efficiency of the products) on basic operational parameters (switching period, electric current density, channel length, substrate inlet concentration) were analyzed.

Biotransformations based on application of immobilized enzymes are frequently used in industrial production of pharmaceuticals, food products, and bulk chemicals. There is, however, a wide range of high-value added products that are produced by means of immobilized enzymes in quite low quantities. These products can be obtained in an inexpensive and simple way using a new kind of manufacturing devices: micro(bio)reactors. The microreactor systems are utilized in many applications ranging from inorganic catalytic reactions with high heat production rates, where system miniaturization brings about strong improvement of heat removal, to biochemical and biological applications. The microsystems in biochemical and biological applications enable to obtain huge amount of data (*e.g.* for screening of biologically active substances) that can be produced by parallel processing [1, 2]. The unique properties of the micro(bio)reactors result from their ability to combine a large number of components and functions within small volume.

An electroosmotic flux is commonly adopted in microreaction systems for fluid transport. The electroosmotic flux can be easily controlled by intensity of an externally imposed electric field and both electrically charged and uncharged solutes can be transported [3]. Pronounced effects of the electroosmotic and electrophoretic transport of reaction components

within a gel with immobilized enzyme on enzyme reactions in macro- and microreactor systems were demonstrated in our previous papers [4, 5]. Certain aspects of a product-inhibited enzyme reaction performed in a microreactor—separator system with the enzyme and adsorbent attached to the channel walls were also studied by Štěpánek *et al.* in [6] where the benefits of the system periodic operation were pointed out.

Mathematical modelling of selected operational aspects of the enzymatic microreactor with electroosmotic pumping of the reaction mixture (that is used as a new tool in capillary electrochromatography [7]) where simultaneous substrate-inhibited enzyme reaction and separation of reaction components *via* adsorption take place is the subject of this paper.

THEORETICAL

Microbioreactor—Separator

A microreactor—separator system considered in this paper is schematically depicted in Fig. 1. Main part of the reactor is a thin channel (CH) filled with a hydrophilic gel (*e.g.* polyacrylamide, agarose, alginate) with the entrapped enzyme and dispersed microparticulate adsorbent. The flow-through substrate well (S) delivers substrate (and buffers) solution to the

*Presented at the 28th International Conference of the Slovak Society of Chemical Engineering, Tatranské Matliare, 21–25 May 2001.

**The author to whom the correspondence should be addressed.

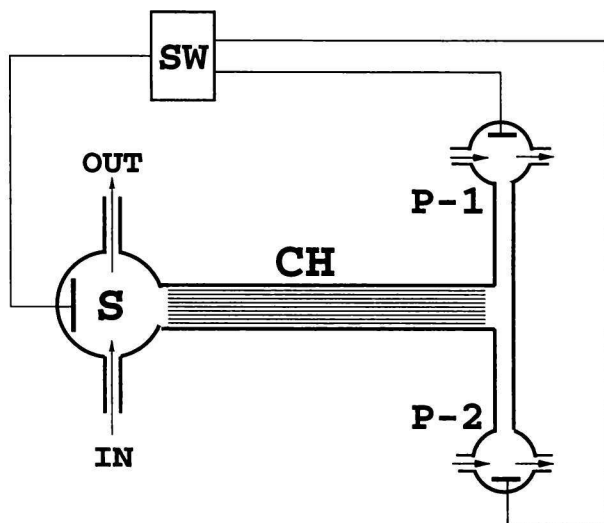


Fig. 1. Schematic depiction of microbioreactor—separator. CH – channel filled with a hydrophilic gel with immobilized enzyme and with dispersed adsorbent; S – substrate well; P-1, P-2 – product wells; SW – channel switch.

gel boundary. A periodic (pulsed) switching of substrate concentration (substrate “ON” and “OFF” periods) in the substrate well is supposed. The reaction period and the separation period of reactor performance therefore periodically alternate. The substrate within the gel is transported *via* molecular diffusion and electroosmosis. The simultaneous enzyme reaction and reaction components separation (*via* adsorption) take place within the gel. The gel-filled channel branches to the outlet channels terminating in product wells (P-1, P-2). Electrodes located in the substrate well and in the product wells allow for switching of the electroosmotic fluid flow to selected outlet well by means of channel switch (SW). The entire microbioreactor—separator system is manufactured in an inert support matrix (typically glass) [1].

Mathematical Model

An enzyme reaction with substrate inhibition including only nonionic reaction components is chosen for modelling. The enzyme (E) converts nonionic substrate (S) to two nonionic products (G, F)



differing in their adsorption parameters. Sucrose hydrolysis by invertase [8] is an example of such reaction. The mathematical model of the enzymatic separating microreactor consists of mass balances of all reaction components both in liquid and solid phases (the adsorbent), enthalpy balance, and equation describing enzyme inactivation. Temperature dependences of reaction rate and enzyme inactivation rate are involved in the model. Hydrodynamic convection in

the gel-filled channel is not considered as no pressure difference across the channel is supposed. The reaction-separation channel of the reactor was considered as spatially one-dimensional system (radial gradients were neglected) with the spatial coordinate z identical to the axis of the channel (the channel diameter is small compared to its length, δ).

The mass balance equation of component i in liquid phase (within the gel pores) in the channel is

$$\frac{\partial c_i}{\partial \tau} = -\nabla \left(j_i^d + \frac{j_i^o}{\varepsilon} \right) - \frac{1-\varepsilon}{\varepsilon} \frac{\partial q_i}{\partial \tau} + \nu_i r \quad (i \equiv S, G, F) \quad (1)$$

where c_i is the concentration of component i in liquid phase, τ is time, ε is the void fraction of the gel in the channel (volume of the gel without adsorbent particles), q_i is the concentration of component i in solid phase and ν_i is the stoichiometric coefficient of component i . The second term on the right-hand side represents the accumulation of the adsorbed component in the solid phase and the last term is the reaction rate for the component i . The diffusional (j_i^d) and electroosmotic (j_i^o) fluxes in eqn (1) are given as

$$j_i^d = -D_i \nabla c_i \quad j_i^o = k_{io} i c_i \quad (2)$$

where D_i is the diffusion coefficient of the component i and k_{io} is an electroosmotic coupling coefficient [2–5].

The mass balance equations for the reaction components in solid phase (the adsorbent), assuming the linear adsorption isotherm and the rate of adsorption/desorption expressed by the linear driving force law, are

$$\frac{\partial q_i}{\partial \tau} = k_a a (K_{ai} c_i - q_i) \quad (3)$$

where $k_a a$ is the mass transfer coefficient and K_{ai} is the adsorption equilibrium constant of the component i .

The enthalpy balance includes heat accumulation in the channel, heat conduction, electroosmotic heat convection, heat production due to the enzyme reaction, Joule heating, and heat transfer at the channel surface (external cooling or heating)

$$\rho c_p \frac{\partial T}{\partial \tau} = \lambda \nabla^2 T - \rho c_p k_{io} i \nabla T + (-\Delta H_R r) + \frac{i^2}{\kappa \varepsilon^2} + \alpha (T_c - T) A_v \quad (4)$$

where ρ is the density, c_p specific heat capacity, T intrachannel temperature, λ heat conductivity, ΔH_R reaction heat, i electric current density, κ electrolytic conductivity, α heat transfer coefficient, T_c channel wall (cooling) temperature, and A_v surface to volume ratio. Considering one-dimensional geometry and introducing dimensionless variables: spatial coordinate $\zeta = z/\delta$, time $\theta = \tau D_S/\delta^2$, liquid-phase concentration $C_i = c_i/c_S^{\text{in}}$, solid-phase concentration $Q_i = q_i/c_S^{\text{in}}$

and intrachannel temperature $\Theta = T/T_{\text{bdr}}$, the model equations can be converted to the following dimensionless form:

The mass balance equations in dimensionless form for components in liquid phase are (cf. e.g. Příbyl et al. [5])

$$\frac{\partial C_i}{\partial \theta} = \frac{D_i}{D_S} \frac{\partial^2 C_i}{\partial \zeta^2} - Pe_o \frac{\partial C_i}{\partial \zeta} - \frac{1-\varepsilon}{\varepsilon} Bi_a (K_{ai} C_i - Q_i) + \varepsilon \nu_i Da \quad (5)$$

The dimensionless mass balance equations for components in solid phase (the adsorbent) are

$$\frac{\partial Q_i}{\partial \theta} = Bi_a (K_{ai} C_i - Q_i) \quad (i \equiv S, F, G) \quad (6)$$

and the enthalpy balance equation in dimensionless form is

$$\frac{\partial \Theta}{\partial \theta} = Le \frac{\partial^2 \Theta}{\partial \zeta^2} - Pe_o \frac{\partial \Theta}{\partial \zeta} + \frac{Da_o}{\varepsilon^2} + \varepsilon Da_H + Bi_H \left(\frac{T_c}{T_{\text{bdr}}} - \Theta \right) \quad (7)$$

Dimensionless parameters: Peclet number Pe_o , Biot number for adsorption Bi_a , Damköhler number for enzyme reaction Da , Damköhler number for heat production by enzyme reaction Da_H , Biot number for heat transfer Bi_H , Lewis number Le , and Damköhler number for heat production due to Joule heating Da_o are defined by the following relations

$$Pe_o = \frac{k_{io} i \delta}{\varepsilon D_S} \quad Bi_a = \frac{k_a a \delta^2}{D_S} \quad Da = \frac{\delta^2}{c_S^{\text{in}} D_S} r \quad Da_H = \frac{\delta^2 (-\Delta H_R)}{\rho c_p D_S T_{\text{bdr}}} r \quad (8)$$

$$Bi_H = \frac{\alpha \delta^2 A_V}{\rho c_p D_S} \quad Le = \frac{\lambda}{\rho c_p D_S} \quad Da_o = \frac{i^2 \delta^2}{\rho c_p \kappa D_S T_{\text{bdr}}} \quad (9)$$

The reaction rate of enzyme reaction r involves substrate inhibition and is given by the relation (dimensional) [8]

$$r = \frac{k_1 w_E c_S}{1 + k_2 c_S + k_3 c_S^2} \quad (10)$$

where c_S is the substrate concentration, w_E enzyme concentration, and k_1, k_2, k_3 are kinetic parameters (k_1 is supposed as temperature-dependent according to Arrhenius relation [8]).

The mass balance equation for dimensionless concentration of the active enzyme w_E , assuming the first-order kinetics of the enzyme inactivation and Arrhenius form of the dependence of inactivation rate constant k_d on temperature, is

$$\frac{dw_E}{d\theta} = -\frac{\delta^2 k_d^{\text{ref}} w_E}{D_S} \exp \left[-\frac{\Delta E_d}{RT_{\text{bdr}}} \left(\frac{1}{\Theta} - \frac{1}{\Theta^{\text{ref}}} \right) \right] \quad (11)$$

where ΔE_d is the activation energy of enzyme inactivation and R is universal gas constant.

Numerical Methods

Spatial derivatives in dimensionless model equations were replaced by finite differences and the resulting sets of ordinary differential equations were solved using the moving grid algorithm-based software package MOVGRD (Blom and Zegeling [9]) in order to get temporal evolution of the reaction component concentrations, the active enzyme concentration, and the temperature within the microreactor–separator channel. The values of model parameters used in simulations are listed in Table 1.

Zero concentrations of the substrate and both reaction products along the entire channel length were considered as initial conditions for eqns (5) and (6)

$$C_i(\theta = 0, 0 < \zeta < 1) = 0 \quad (i \equiv S, F, G) \quad (12)$$

Table 1. Values of Model Parameters

Parameter	Value	Unit	Parameter	Value	Unit
A_V	2000	m^{-1}	K_{aF}	0.8	–
c_p	4187	$\text{J kg}^{-1} \text{K}^{-1}$	K_{aG}	0.2	–
D_F	10.0×10^{-10}	$\text{m}^2 \text{s}^{-1}$	K_{aS}	0.0	–
D_G	10.0×10^{-10}	$\text{m}^2 \text{s}^{-1}$	R	8.314	$\text{J mol}^{-1} \text{K}^{-1}$
D_S	7.0×10^{-10}	$\text{m}^2 \text{s}^{-1}$	T_{bdr}	343.15	K
E_R	35000	J mol^{-1}	T_c	343.15	K
E_d	250000	J mol^{-1}	w_{E0}	50.0	kg m^{-3}
ΔH_R	13500	J mol^{-1}	X_{ON}	0.05	–
k_{aa}	0.5	s^{-1}	α	2000	$\text{W m}^{-2} \text{K}^{-1}$
k_d^{ref}	1.0×10^{-7}	s^{-1}	ε	0.4	–
k_{io}	-5.0×10^{-8}	$\text{m}^3 \text{A}^{-1} \text{s}^{-1}$	κ	0.5	S m^{-1}
k_1^{ref}	0.1	$\text{m}^3 \text{kg}^{-1} \text{s}^{-1}$	λ	0.65	$\text{W m}^{-1} \text{K}^{-1}$
k_2	3.0×10^{-3}	$\text{m}^3 \text{mol}^{-1}$	ρ	1200	kg m^{-3}
k_3	5.0×10^{-4}	$\text{m}^6 \text{mol}^{-2}$	θ_{sw}	0.005	–

Flat initial temperature profile ($T = T_{\text{bdr}}$) in the channel was used as initial condition for the enthalpy balance (7), *i.e.* in dimensionless form

$$\Theta(\theta = 0, 0 < \zeta < 1) = 1 \quad (13)$$

Homogeneous distribution of the enzyme in the channel was used as initial condition for eqn (11)

$$\omega_E(\theta = 0, 0 < \zeta < 1) = 1 \quad (14)$$

Following boundary conditions were used

$$C_S = (\theta, \zeta = 0) = C_S^{\text{in}} \quad (15)$$

$$\frac{\partial C_i(\theta, \zeta = 0)}{\partial \zeta} = 0, \quad i \equiv S, F, G$$

$$\frac{\partial C_i(\theta, \zeta = 1)}{\partial \zeta} = 0, \quad i \equiv S, F, G \quad (16)$$

$$\Theta(\theta, \zeta = 0) = \Theta(\theta, \zeta = 1) = 1$$

RESULTS AND DISCUSSION

The effects of basic operational parameters of the microreactor—separator system (electric current density, reaction channel length, substrate inlet concentration) on its reaction and separation efficiency were studied. An example of spatio-temporal evolution of the intrachannel component concentrations in the liquid phase is shown in Fig. 2. The substrate (dosed to the channel entry in a form of short concentration pulses, *cf.* Fig. 3) is transported into the gel with immobilized enzyme and is completely consumed by the reaction before it reaches half the length of the channel. The products formed are transported *via* diffusion and electroosmotic flux to the channel outlet. Due to the different sorption strength of the products F and G on adsorbent particles in the gel, the product separation occurs.

An example of reaction products separation is shown in Fig. 3, where also the substrate-pulsed input to the channel inlet is depicted. Satisfactory separation of products G and F is obvious. The efficiency of reaction products separation was quantified by the efficiency of separation E_S^{GF} of components G and F defined as [10]

$$E_S^{\text{GF}} = \frac{|\bar{t}_G - \bar{t}_F|}{\sqrt{s_G s_F}} \quad (17)$$

where \bar{t}_i and s_i are the mean elution times and peak widths of respective components at the channel outlet.

Dependence of the separation efficiency on electric current density i , channel length δ , and substrate inlet concentration C_S^{in} was analyzed (Fig. 4). The influence of electric current intensity i on the E_S^{GF} value was

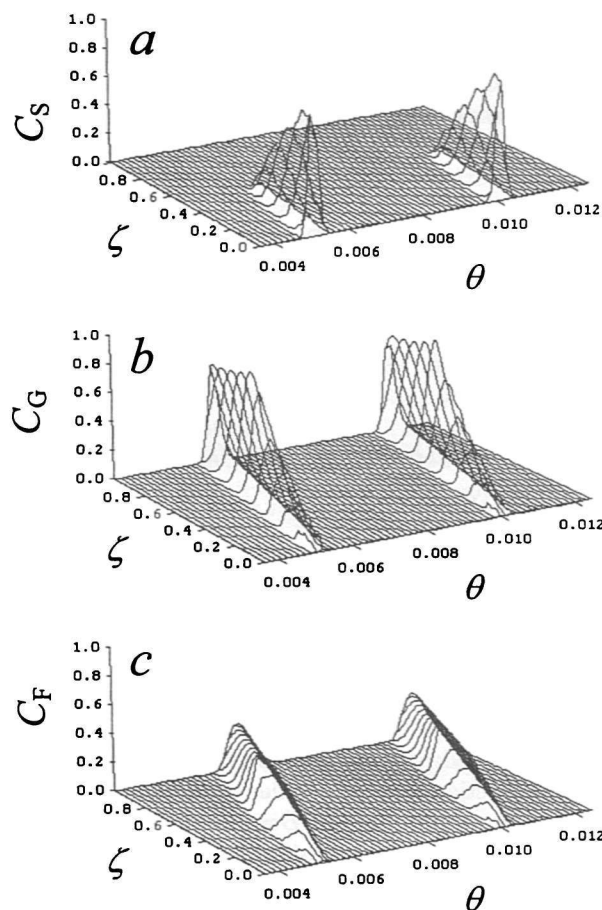


Fig. 2. Spatio-temporal evolution of dimensionless concentrations of reaction components in liquid phase in reaction channel. a) Substrate S; b) product G; c) product F. Parameters: channel length $\delta = 1 \times 10^{-2}$ m; electric current density $i = -500 \text{ A m}^{-2}$; substrate inlet concentration $C_S^{\text{in}} = 1 \text{ kmol m}^{-3}$; total period of substrate concentration switching $\theta_{\text{sw}} = 0.005$; ratio of substrate "ON" sub-period duration to total switching period $X_{\text{ON}} = 0.05$.

studied for negative values of i , when the electroosmotic flux supports the reaction components transport in the channel towards the product well. The E_S^{GF} value increases with increasing electric current intensity up to $i \approx -225 \text{ A m}^{-2}$, where it reaches its maximum value of about 4.93. The increase of E_S^{GF} value in Fig. 4a is due to deceleration of the electroosmotic flux with increasing electric current density (it should be kept in mind that the values of i are negative). The deceleration of the electroosmotic flux, *i.e.* the deceleration of the rate of products transport out of the channel, results in improved separation of the products G and F because of extension of the separation time. Positive electric current densities cannot be applied to the channel as then the electroosmotic flux direction is oriented towards the substrate well and no reaction products can be transported to any of the product wells.

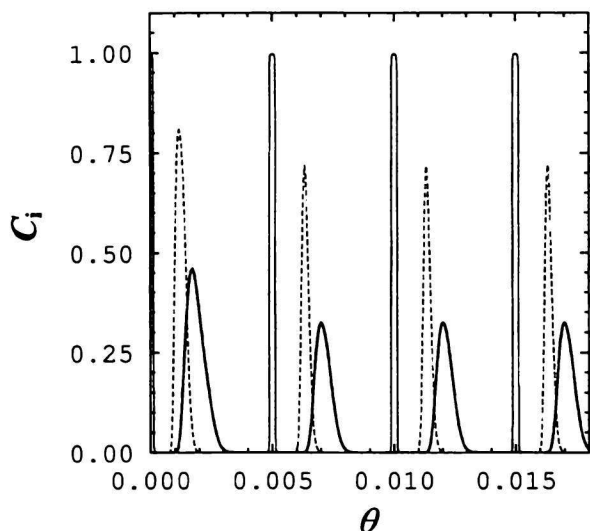


Fig. 3. Dimensionless inlet substrate concentration S (—) and product outlet concentrations F (—) and G (---). Parameter values as in Fig. 2.

The channel length (*i.e.* the available separation distance) also remarkably influences the efficiency of separation (Fig. 4b). It is obvious that the longer the separation distance δ , the greater the E_S^{GF} value (the better separation of products G and F). The increase of the E_S^{GF} with the channel length δ from 5 to 15 mm is, however, only about 30 % contrary to the manifold increase shown in Fig. 4a. The separation efficiency control *via* adjustments of the electric current density represents therefore an appropriate tool for microreactor—separator management.

With increasing value of the substrate inlet concentration c_S^{in} the E_S^{GF} value decreases (Fig. 4c). High values of the substrate inlet concentration ($c_S^{in} = 1500 \text{ mol m}^{-3}$) bring about substantial deceleration of the enzyme reaction (due to substrate inhibition). Then, the unreacted substrate scatters over a wide portion of the channel and nonzero value of the substrate liquid-phase concentration at the channel outlet may arise. This regime of the system performance is obviously unacceptable in practical systems. Therefore, the inlet substrate concentration must be properly set (with regard to the channel length and the electric current density values) in order to attain both the complete substrate conversion and the reaction products separation.

CONCLUSION

The mathematical model of the enzymatic separating microreactor presented in this paper has been found a suitable tool for analysis of various aspects of the microreactor performance. The influence of selected parameters of the mathematical model (electric current density, length of the microreactor—separator

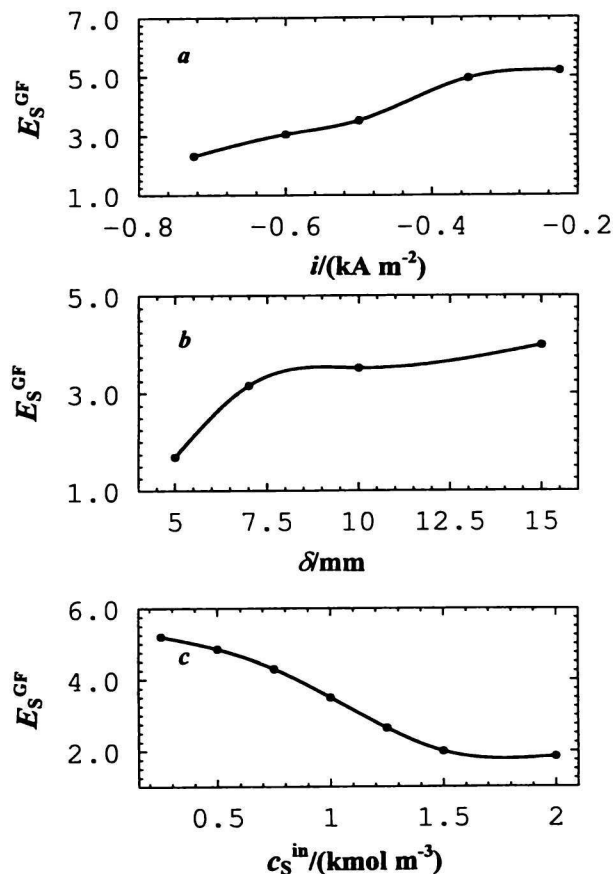


Fig. 4. Efficiency of the reaction products separation E_S^{GF} at reactor outlet as a function of a) electric current density i (at constant channel length $\delta = 1 \times 10^{-2} \text{ mm}$ and substrate inlet concentration $c_S^{in} = 1 \text{ kmol m}^{-3}$), b) channel length δ (at constant electric current density $i = -500 \text{ A m}^{-2}$ and substrate inlet concentration $c_S^{in} = 1 \times 10^3 \text{ mol m}^{-3}$), and c) substrate inlet concentration c_S^{in} (at constant channel length $\delta = 1 \times 10^{-2} \text{ mm}$ and electric current density $i = -500 \text{ A m}^{-2}$). Parameters: total period of substrate concentration switching $\theta_{sw} = 0.005$; ratio of substrate “ON” sub-period duration to total switching period $X_{ON} = 0.05$.

channel, substrate inlet concentration) on efficiency of the product separation is demonstrated. The feasibility of supposed configuration of the microreaction—separation system with simultaneous enzyme reaction, adsorption of the reaction components, and transport of the reaction components driven by electroosmotic flux was clearly confirmed.

Acknowledgements. Financial support of this project by the Grant Agency of the Czech Republic (Grant No. 104/01/1319) is gratefully acknowledged.

SYMBOLS

A_V	surface to volume ratio	m^{-1}
c	liquid-phase concentration	mol m^{-3}
c_p	specific heat capacity	$\text{J kg}^{-1} \text{K}^{-1}$

C	dimensionless liquid-phase concentration	
D	diffusion coefficient	$\text{m}^2 \text{s}^{-1}$
E_R	activation energy of enzyme reaction	J mol^{-1}
ΔE_d	activation energy of enzyme inactivation	J mol^{-1}
E_S^{GF}	efficiency of separation	
ΔH_R	reaction heat	J mol^{-1}
i	electric current density	A m^{-2}
j_i^d	intensity of diffusional flux of component i	$\text{mol m}^{-2} \text{s}^{-1}$
j_i^o	intensity of electroosmotic flux of component i	$\text{mol m}^{-2} \text{s}^{-1}$
$k_a a$	mass transfer coefficient	s^{-1}
k_d	rate constant of enzyme inactivation	s^{-1}
k_{io}	electroosmotic coupling coefficient	$\text{m}^3 \text{A}^{-1} \text{s}^{-1}$
k_1	kinetic parameter in eqn (10)	$\text{m}^3 \text{kg}^{-1} \text{s}^{-1}$
k_2	kinetic parameter in eqn (10)	$\text{m}^3 \text{mol}^{-1}$
k_3	kinetic parameter in eqn (10)	$\text{m}^6 \text{mol}^{-2}$
K_a	adsorption equilibrium constant	
q	solid-phase concentration	mol m^{-3}
Q	dimensionless solid-phase concentration	
r	reaction rate	$\text{mol m}^{-3} \text{s}^{-1}$
R	universal gas constant	$\text{J mol}^{-1} \text{K}^{-1}$
s	peak width of component at the channel outlet	s^{-1}
\bar{t}	mean elution time of component	s^{-1}
T	intrachannel temperature	K
T_c	channel wall (cooling) temperature	K
w_E	enzyme concentration	kg m^{-3}
X_{ON}	fraction of substrate "ON" sub-period	
z	spatial coordinate	m
α	heat transfer coefficient	$\text{W m}^{-2} \text{K}^{-1}$
δ	length of the channel	m
ε	void fraction of the gel in the channel	
Θ	dimensionless intrachannel temperature	
κ	electrolytic conductivity	S m^{-1}
λ	heat conductivity	$\text{W m}^{-1} \text{K}^{-1}$
ν	stoichiometric coefficient	
ζ	dimensionless spatial coordinate	
ρ	density	kg m^{-3}
τ	time	s
θ	dimensionless time	

ω dimensionless enzyme concentration

Subscripts

o	initial
bdr	boundary
E	enzyme
F, G	products
i	component i
sw	substrate concentration switching
S	substrate

Superscripts

d	diffusion
in	inlet value
o	electroosmosis
ref	reference value

REFERENCES

1. Ehrfeld, W., Hessel, V., Kieselwater, S., Löwe, H., Richter, Th., and Schiewe, J., *Implementation of Microreaction Technology in Process Engineering in Proceedings of IMRET 3*, 3rd International Conference on Microreaction Technology, Frankfurt, 1999.
2. Fletcher, P. D. I., Haswell, S. J., and Paunov, V. N., *Analyst* 124, 1273 (1999).
3. Chang, Y.-H. D., Grodzinsky, A. J., and Wang, D. I. C., *Biotechnol. Bioeng.* 48, 149 (1995).
4. Přibyl, M., Hasal, P., and Marek, M., *Chem. Biochem. Eng. Q.* 12, 141 (1998).
5. Přibyl, M., Chmelíková, R., Hasal, P., and Marek, M., *Chem. Eng. Sci.* 56, 433 (2001).
6. Štěpánek, F., Kubíček, M., Marek, M., and Adler, P. M., *Chem. Eng. Sci.* 54, 1493 (1999).
7. Dittman, M. M. and Rozing, G., *J. Microcolumn Sep.* 9, 399 (1997).
8. Hasal, P., Vojtíšek, V., Čejková, A., Kleczek, P., and Kofroňová, O., *Enzyme Microb. Technol.* 14, 221 (1992).
9. Blom, J. G. and Zegeling, P. A., *ACM Trans. Math. Soft.* 20, 194 (1994).
10. Cheng, Y. L. and Lee, T. Y., *Biotechnol. Bioeng.* 40, 498 (1992).